Computing Minimum-Power Dipole Solutions for Interdipole Forces Using Nonlinear Constrained Optimization With Application to Electromagnetic Formation Flight

Jake J. Abbott, Joseph B. Brink, and Braxton Osting

***Abstract*—Electromagnetic formation flight (EMFF) denotes a method of formation flight control in which a cluster of spacecraft are equipped with controllable magnetic dipoles for coordination of their relative positions using interdipole forces. We present a method for finding a minimum-power dipole solution for a given set of desired interdipole forces. We approach this nonlinear constrained optimization problem using sequential quadratic programming, which requires a Jacobian relating changes in the dipoles to changes in forces, as well as the gradient and Hessian of a Lagrangian function. We derive compact analytic solutions for all three of these quantities, using linear-algebraic representations and vector calculus, which can be implemented numerically with a small set of simple functions. Our approach does not rely on arbitrary parameterizations as have prior approaches, and the structure enables further analysis of numerical conditioning and convergence. We conduct numerical simulations, using a number of configurations relevant to EMFF, to verify the method and characterize its performance when numerical routines are randomly initialized, which can serve as a benchmark against which future improvements can be quantified. The method presented may have other uses beyond EMFF, including being applied to new classes of modular magnetic systems.**

***Index Terms*—Cellular and modular robots, distributed robot systems, optimization and optimal control, space robotics.**

I. Introduction

ELECTROMAGNETIC formation flight (EMFF) denotes a method in which spacecraft within a cluster are equipped with controllable magnetic dipoles that are used to control their relative positions by generating interdipole forces, typically in conjunction with reaction wheels to control their orientations (which is typically considered a solved, decoupled, and more energetically efficient problem) [1]. EMFF models typically assume that each spacecraft has three orthogonal electromagnetic coils to generate the controllable dipole. In contrast to the use of traditional propellants, EMFF will not interfere with sensitive optical instruments and can utilize renewable solar energy. With EMFF alone it is not possible to affect the center-of-mass of the cluster. However, this is not of concern for the primary motivating application of EMFF: sparse-aperture interferometry telescopes. A number of configurations of such systems have been proposed and investigated to date, including three spacecraft that maintain an equilateral triangle [1]–[5], and three or five spacecraft that maintain a collinear arrangement [1], [4], [6]–[8], while the interspacecraft separation distances and angular velocity of the cluster are controlled. In addition, the complete dynamic control problem has been solved for two spacecraft [9]–[11], which can be useful for inspection tasks [8]. The motivation and feasibility of EMFF for the above applications has been discussed in detail in many of the cited works. In addition, the techniques and technology of EMFF may have other uses [8], including being applied more broadly to new classes of modular and fractionated space systems [12]–[15].

Given a set of desired forces on each spacecraft (generated by a higher-level motion planner to accomplish to dynamic trajectory or closed-loop servoing task), multiple solutions often exist for the set of dipoles that will achieve those forces. Schweighart [16] found a solution given an arbitrary set of spacecraft positions and desired forces. He showed that any set of desired forces can be achieved, up to saturation, provided the forces sum to zero (since the center-of-mass of the ensemble cannot be moved). His solution involves setting one of the dipoles to an arbitrary (nonzero) value and solving for the remaining dipoles by solving a set of polynomial equations, and then evolving the arbitrarily set dipole using numerical optimization techniques to minimize some cost function (he chose to minimize the magnetic torque that was generated as a side effect of the magnetic force). Although [16] makes a number of important contributions to the topic of EMFF, the numerical algorithm itself is challenging to implement and the inner workings can be difficult to follow.

In this paper, we provide an alternate method for computing the magnetic dipoles for a given set of interdipole forces.

Manuscript received August 19, 2016; accepted January 5, 2017. Date of publication January 25, 2017; date of current version February 9, 2017. This paper was recommended for publication by Associate Editor E. Papadopoulos and Editor K. Lynch upon evaluation of the reviewers' comments. This work was supported by the National Aeronautics and Space Administration under Grant NNX13AL46H.

J. J. Abbott is with the Department of Mechanical Engineering and the Robotics Center, University of Utah, Salt Lake City, UT 84112 USA (e-mail: jake.abbott@utah.edu).

J. B. Brink is with the Department of Mechanical Engineering, University of Utah, Salt Lake City, UT 84112 USA (e-mail: brink.joey@gmail.com).

B. Osting is with the Department of Mathematics, University of Utah, Salt Lake City, UT 84112 USA (e-mail: osting@math.utah.edu).

Color versions of one or more of the figures in this paper are available online at http://ieeexplore.ieee.org.

Digital Object Identifier 10.1109/LRA.2017.2658727

2377-3766 © 2017 IEEE. Personal use is permitted, but republication/redistribution requires IEEE permission.
See http://www.ieee.org/publications_standards/publications/rights/index.html for more information.

A significant challenge in EMFF is minimizing power consumption, and although (possibly infinitely) many solutions exist, computational studies suggest only a few exist that minimize the power consumed by the electromagnetic coils. We find a solution to minimize the weighted dipoles, which can represent a variety of minimum-power solutions by choosing the weights appropriately. We approach this nonlinear constrained optimization problem using sequential quadratic programming (SQP), which is a second-order method that is known to converge toward a local minimum in fewer iterations than first-order gradient-descent methods [17]. The method requires the calculation of a Jacobian relating differential changes in the dipoles to differential changes in the forces, as well as both the gradient and Hessian of a Lagrangian function. We provide a compact analytic solution for all three of these quantities, using linear-algebraic representations and vector calculus, which can be implemented numerically with a small set of simple functions; this is the principal contribution of our work. For this nonconvex optimization problem, the SQP method only converges to a local minimum, and we conduct an empirical study for several example configurations relevant to EMFF to evaluate our method. Our approach does not rely on arbitrary parameterizations, as have prior approaches [16], and the structure enables further analysis of numerical conditioning and convergence.

A few prior works that address the full flight-planning problem have suggested that sequential quadratic programming could be applied to the EMFF problem [18], [19], but those works have not provided the analytic results for the problem, nor the numerical verification, that we provide in this paper. Here, we do not concern ourselves with *what* forces should be generated, which is a topic governed by dynamics and path-planning concerns beyond the scope of this paper. We also do not address magnetic torque, assuming that orientation is independently controlled with reaction wheels, as is assumed in most prior work in EMFF.

A secondary intent of this paper is to introduce the Robotics & Automation community, within which there has been significant effort in the field of magnetic manipulation over more than a decade, to the related literature from the Aeronautics & Astronautics community. To date, research in these two communities has evolved in parallel and without cross-pollination.

II. Forces Between Magnetic Dipoles

In this section we express the internal forces generated within a set of controllable magnetic dipoles. We express the equations using linear-algebraic techniques, which do not require arbitrary angular parameterizations. This representation forms the foundation for the remainder of the paper.

A. Force Between Two Dipoles

We first review the force between two magnetic dipoles, using the notation and results from [20], which describes the use of a single controllable dipole to manipulate a second permanent-magnet dipole, but also applies to the case where the second dipole is itself controllable.

A controllable magnetic dipole $\mathbf{m}_i \in \mathscr{R}^3$ at location i, in units $\{\mathrm{A{\cdot}m^2}\}$, is a linear function $\mathbb{M}_i$ of three controlled currents, in units $\{\mathrm{A}\}$, stacked in an array $\mathbf{I}_i \in \mathscr{R}^3$:

$$\mathbf{m}_i = \mathbb{M}_i \mathbf{I}_i \tag{1}$$

where $\mathbb{M}_i$, in units $\{\mathrm{m^2}\}$, is typically a diagonal matrix representing orthogonal electromagnets. A dipole generates a magnetic field $\mathbf{b}_{ij} \in \mathscr{R}^3$ at location j, in units $\{\mathrm{T}\}$, modeled by the equation:

$$\mathbf{b}_{ij} = \frac{\mu_0}{4\pi \|\mathbf{p}_{ij}\|^3} \left(3\hat{\mathbf{p}}_{ij}\hat{\mathbf{p}}_{ij}^T - \mathbb{I}\right) \mathbf{m}_i = \mathbb{B}_{ij}\mathbf{m}_i \tag{2}$$

where $\mu_0 = 4\pi \times 10^{-7}$ $\mathrm{T{\cdot}m{\cdot}A^{-1}}$ is the permeability of free space, $\mathbb{I}$ is the identity matrix, $\mathbf{p}_{ij} \in \mathscr{R}^3$ is the position vector from i to j, in units $\{\mathrm{m}\}$, $\hat{\mathbf{p}}_{ij}$ is the normalized unit vector in the direction of $\mathbf{p}_{ij}$, and the matrix $\mathbb{B}_{ij}$, in units $\{\mathrm{m^{-3}}\}$, is a function of $\mathbf{p}_{ij}$. We note that the controllable dipole linearly affects the magnetic field that it generates at each location.

The field generated by dipole $\mathbf{m}_i$ imparts a force $\mathbf{f}_{ij} \in \mathscr{R}^3$, in units $\{\mathrm{N}\}$, on a second magnetic dipole $\mathbf{m}_j$ at location j:

$$\mathbf{f}_{ij} = \mathbb{F}_{ij}\mathbf{m}_i \tag{3}$$

where

$$\mathbb{F}_{ij} = \frac{3\mu_0}{4\pi\|\mathbf{p}_{ij}\|^4}\left(\mathbf{m}_j\hat{\mathbf{p}}_{ij}^T + \hat{\mathbf{p}}_{ij}\mathbf{m}_j^T + \left(\hat{\mathbf{p}}_{ij}^T\mathbf{m}_j\right)\left(\mathbb{I} - 5\hat{\mathbf{p}}_{ij}\hat{\mathbf{p}}_{ij}^T\right)\right). \tag{4}$$

The matrix $\mathbb{F}_{ij}$, in units $\{\mathrm{N{\cdot}A^{-1}{\cdot}m^{-2}}\}$, is a function of $\mathbf{p}_{ij}$ and $\mathbf{m}_j$. We note that $\mathbf{f}_{ij}$ linearly depends on $\mathbf{m}_i$. If all vectors are expressed with respect to a common coordinate frame, it is easy to show that $\mathbf{f}_{ij} = -\mathbf{f}_{ji}$ (i.e., forces between dipoles are "equal and opposite", as expected).

B. Forces Between an Arbitrary Number of Dipoles

For a set of N magnetic dipoles, it is not possible to control the forces applied to all of the dipoles independently. We will structure the problem as generating a set of desired forces on the first $N-1$ of those dipoles, defined with respect to a common reference frame centered at the location of the N^{th} dipole, with the understanding that equal and opposite forces will be generated on the N^{th} dipole.

We will use the input $\mathbf{M} \in \mathscr{R}^{3N}$, which is an array comprising the N controllable dipole vectors, to generate the output $\mathbf{F} \in \mathscr{R}^{3(N-1)}$, which is an array comprising the force vectors on the first $N-1$ dipoles:

$$\mathbf{M} = \begin{bmatrix} \mathbf{m}_1 \\ \vdots \\ \mathbf{m}_N \end{bmatrix}, \quad \mathbf{F} = \begin{bmatrix} \mathbf{F}_1 \\ \vdots \\ \mathbf{F}_{N-1} \end{bmatrix} \tag{5}$$

where the total force $\mathbf{F}_j$ on dipole j is the sum of all of the dipole-dipole interaction forces:

$$\mathbf{F}_j = \sum_{i=1}^{N} \mathbf{f}_{ij} \tag{6}$$

with $\mathbf{f}_{ij}$ defined in (3), and where we define $\mathbf{f}_{jj} = \mathbf{0}$ (i.e., there is no force of a dipole on itself).

It is understood that the force on the N^{th} dipole is constrained by the forces on the first $N-1$:

$$\sum_{i=1}^{N} \mathbf{F}_i = 0 \quad \longrightarrow \quad \mathbf{F}_N = -\sum_{i=1}^{N-1} \mathbf{F}_i \tag{7}$$

Utilizing the fact that $\mathbf{f}_{ij} = -\mathbf{f}_{ji}$, the force array $\mathbf{F}$ can be expressed in two equally valid forms:

$$\begin{aligned}\mathbf{F} &= \begin{bmatrix} \mathbb{O} & \mathbb{F}_{21} & \dots & \mathbb{F}_{(N-1)1} & \mathbb{F}_{N1} \\ \mathbb{F}_{12} & \mathbb{O} & \dots & \mathbb{F}_{(N-1)2} & \mathbb{F}_{N2} \\ \vdots & \vdots & \ddots & \vdots & \vdots \\ \mathbb{F}_{1(N-1)} & \mathbb{F}_{2(N-1)} & \dots & \mathbb{O} & \mathbb{F}_{N(N-1)} \end{bmatrix} \mathbf{M} \\ &= \begin{bmatrix} -\sum_{i=1}^{N} \mathbb{F}_{1i} & \mathbb{O} & \dots & \mathbb{O} & \mathbb{O} \\ \mathbb{O} & -\sum_{i=1}^{N} \mathbb{F}_{2i} & \dots & \mathbb{O} & \mathbb{O} \\ \vdots & \vdots & \ddots & \vdots & \vdots \\ \mathbb{O} & \mathbb{O} & \dots & -\sum_{i=1}^{N} \mathbb{F}_{(N-1)i} & \mathbb{O} \end{bmatrix} \mathbf{M}\end{aligned} \tag{8}$$

where $\mathbb{O}$ is a square zero matrix, and we define $\mathbb{F}_{ii} = \mathbb{O}$.

III. Solving the Constrained Optimization

A. Problem Statement

Our goal is to find a weighted-dipole solution that minimizes a weighted L^2-norm for a given set of desired internal forces between a set of N controllable magnetic dipoles. We assume the desired forces are provided by some external planner or closed-loop controller. We say "a" solution, rather than "the" solution, because there are always at least two solutions that achieve the minimum dipole. For a set of free-floating bodies, it is not possible to change the momentum of the center-of-mass of the bodies using only internal forces, so we will structure the problem as generating a set of desired forces on the first $N-1$ of those dipoles, defined with respect to a common reference frame centered at the location of the N^{th} dipole, with the understanding that equal and opposite forces will be generated on the N^{th} dipole.

We will use the input $\mathbf{M}$ to generate the output $\mathbf{F}$, defined in (5), with the goal of achieving some desired output $\mathbf{F}_{\text{d}}$:

$$\mathbf{F}_{\text{d}} = \begin{bmatrix} \mathbf{F}_{\text{d}1} \\ \vdots \\ \mathbf{F}_{\text{d}(N-1)} \end{bmatrix}. \tag{9}$$

Given a desired force $\mathbf{F}_{\text{d}}$, our goal is to solve the following nonlinear constrained optimization problem:

$$\begin{aligned} \min_{\mathbf{M}} \quad & \frac{1}{2}\mathbf{M}^T \mathbb{W} \mathbf{M} \\ \text{s.t.} \quad & \mathbf{F}(\mathbf{M}) = \mathbf{F}_{\text{d}} \end{aligned} \tag{10}$$

where $\mathbb{W} \in \mathscr{R}^{3N \times 3N}$ is a diagonal weighting matrix with positive entries, comprising N diagonal weighting submatrices associated with each of the individual dipoles: $\mathbb{W} = \text{diag}\{\mathbb{W}_1, \dots, \mathbb{W}_N\}$.

B. Sequential Quadratic Programming

The Lagrangian function $\mathscr{L} : \mathscr{R}^{3N} \times \mathscr{R}^{3(N-1)} \to \mathscr{R}$ is:

$$\mathscr{L} = \frac{1}{2}\mathbf{M}^T \mathbb{W} \mathbf{M} + \boldsymbol{\lambda}^T (\mathbf{F} - \mathbf{F}_{\text{d}}) \tag{11}$$

where $\boldsymbol{\lambda} \in \mathscr{R}^{3(N-1)}$ is an array of Lagrange multipliers, which we will maintain as $N-1$ independent vectors of Lagrange multipliers associated with the $N-1$ force vectors:

$$\boldsymbol{\lambda} = \begin{bmatrix} \boldsymbol{\lambda}_1 \\ \vdots \\ \boldsymbol{\lambda}_{N-1} \end{bmatrix}. \tag{12}$$

SQP, applied to our problem, is as follows [17]. Given some initial value of $\mathbf{M}[\ell]$ and $\boldsymbol{\lambda}[\ell]$ at iteration ℓ, the update for $\mathbf{M}[\ell+1] = \mathbf{M}[\ell] + \Delta\mathbf{M}$ and $\boldsymbol{\lambda}[\ell+1]$ can be found by solving the system of equations

$$\begin{bmatrix} \mathbb{H}[\ell] & \mathbb{J}^T[\ell] \\ \mathbb{J}[\ell] & \mathbb{O} \end{bmatrix} \begin{bmatrix} \Delta\mathbf{M} \\ \boldsymbol{\lambda}[\ell+1] \end{bmatrix} = \begin{bmatrix} -\nabla_{\mathbf{M}} \left(\frac{1}{2}\mathbf{M}^T \mathbb{W} \mathbf{M}\right) \\ -(\mathbf{F} - \mathbf{F}_{\text{d}}) \end{bmatrix} \tag{13}$$

for example, using Gaussian elimination, where $\nabla_{\mathbf{M}}(\frac{1}{2}\mathbf{M}^T \mathbb{W} \mathbf{M})$ is the gradient of the objective function with respect to $\mathbf{M}$, $\mathbb{J}$ is the Jacobian of the constraint $\mathbf{F} - \mathbf{F}_{\text{d}}$ with respect to $\mathbf{M}$, and $\mathbb{H}$ is the Hessian of the Lagrangian with respect to $\mathbf{M}$. Although numerical methods exist to approximate each of the various quantities of interest in (13), we explicitly solve for each quantity below, which is an important contribution to the characterization and efficient implementation of this method, but has not been done previously.

First, we calculate the gradient of the objective function with respect to the $3N$ independent variables in $\mathbf{M}$ as:

$$\nabla_{\mathbf{M}} \left(\frac{1}{2}\mathbf{M}^T \mathbb{W} \mathbf{M}\right) = \mathbb{W} \mathbf{M} \tag{14}$$

Next, we compute the Jacobian $\mathbb{J} \in \mathscr{R}^{3(N-1) \times 3N}$. Because $\mathbf{F}_{\text{d}}$ can be considered constant throughout the optimization, the Jacobian of the constraint $\mathbf{F} - \mathbf{F}_{\text{d}}$ with respect to $\mathbf{M}$ is equal to the Jacobian of $\mathbf{F}$ with respect to $\mathbf{M}$. We can find this Jacobian $\mathbb{J}$ that relates differential changes in the dipole moments to differential changes in the forces:

$$d\mathbf{F} = \mathbb{J}\, d\mathbf{M} = \begin{bmatrix} \frac{\partial \mathbf{F}}{\partial \mathbf{m}_1} & \dots & \frac{\partial \mathbf{F}}{\partial \mathbf{m}_N} \end{bmatrix} \begin{bmatrix} d\mathbf{m}_1 \\ \vdots \\ d\mathbf{m}_N \end{bmatrix} \tag{15}$$

The partial derivatives in $\mathbb{J}$ can be computed analytically by utilizing the two forms of $\mathbf{F}$ given in (8), and noting that $\mathbb{F}_{ij}$ is

a function of $\mathbf{m}_j$ but not $\mathbf{m}_i$. The resulting Jacobian is

$$\mathbb{J} = \begin{bmatrix} -\sum_{i=1}^{N} \mathbb{F}_{1i} & \mathbb{F}_{21} & \cdots & \mathbb{F}_{(N-1)1} & \mathbb{F}_{N1} \\ \mathbb{F}_{12} & -\sum_{i=1}^{N} \mathbb{F}_{2i} & \cdots & \mathbb{F}_{(N-1)2} & \mathbb{F}_{N2} \\ \vdots & \vdots & \ddots & \vdots & \vdots \\ \mathbb{F}_{1(N-1)} & \mathbb{F}_{2(N-1)} & \cdots & -\sum_{i=1}^{N} \mathbb{F}_{(N-1)i} & \mathbb{F}_{N(N-1)} \end{bmatrix}. \tag{16}$$

Note that once this Jacobian is computed and stored, neither of the two matrices in (8) need to be explicitly computed nor stored, since $\mathbf{F}$ can be computed efficiently using the main diagonal blocks of $\mathbb{J}$.

Finally, we compute the symmetric Hessian $\mathbb{H} \in \mathscr{R}^{3N\times 3N}$:

$$\mathbb{H} = \nabla^2_{\mathbf{MM}}(\mathcal{L}) = \begin{bmatrix} \mathbb{W}_1 & \mathbb{H}_{12} & \cdots & \mathbb{H}_{1N} \\ \mathbb{H}_{21} & \mathbb{W}_2 & \cdots & \mathbb{H}_{2N} \\ \vdots & \vdots & \ddots & \vdots \\ \mathbb{H}_{N1} & \mathbb{H}_{N2} & \cdots & \mathbb{W}_N \end{bmatrix} \tag{17}$$

where the remaining 3×3 matrix blocks are of the form

$$\mathbb{H}_{ij} = \frac{\partial(\mathbb{F}_{ij}^T \boldsymbol{\lambda}_j)}{\partial \mathbf{m}_j} - \frac{\partial(\mathbb{F}_{ij}^T \boldsymbol{\lambda}_i)}{\partial \mathbf{m}_j} \tag{18}$$

and the partial derivatives in (18) have the analytic form

$$\frac{\partial(\mathbb{F}_{ij}^T \boldsymbol{\lambda}_k)}{\partial \mathbf{m}_j} = \frac{3\mu_0}{4\pi\|\mathbf{p}_{ij}\|^4}\Big(\hat{\mathbf{p}}_{ij}\boldsymbol{\lambda}_k^T + \left(\hat{\mathbf{p}}_{ij}^T\boldsymbol{\lambda}_k\right)\mathbb{I} + \left(\mathbb{I} - 5\hat{\mathbf{p}}_{ij}\hat{\mathbf{p}}_{ij}^T\right)\boldsymbol{\lambda}_k\hat{\mathbf{p}}_{ij}^T\Big) \tag{19}$$

where we define $\boldsymbol{\lambda}_N = \mathbf{0}$. Note that only half of the remaining blocks in (17) need to be explicitly computed using (18), due to the known symmetry of the Hessian.

For SQP, we must initialize the $3N$ dipole moments (i.e., N dipole moment vectors) in $\mathbf{M}$ and the $3(N-1)$ Lagrange multipliers in $\boldsymbol{\lambda}$ to seed the update equation (13). If we have the solution to the optimization problem from a previous time step, and our $\mathbf{F}_\mathrm{d}$ has not changed significantly, we use the solution for $\mathbf{M}$ and $\boldsymbol{\lambda}$ from the previous time step as our initial guess for the current time step. If we do not have a solution from a previous time step, we must determine a method to initialize $\mathbf{M}$ and $\boldsymbol{\lambda}$, which could be as simple choosing random values.

C. Choosing the Weighting Matrix

Our objective function in (10) requires a weighting matrix $\mathbb{W}$. We established in (1) that the individual controllable dipoles are linear with respect to the current, so the objective function will be quadratic with respect to current. Let $\mathbb{R}_i \in \mathscr{R}^{3\times 3}$ be a diagonal matrix comprising the individual coil resistances in a given spacecraft (including the series resistances of the power electronics for the individual coils). By choosing the individual weighting matrices in $\mathbb{W}$ as

$$\mathbb{W}_i = 2\mathbb{M}_i^{-T}\mathbb{R}_i\mathbb{M}_i^{-1} \tag{20}$$

and defining $\mathbb{R} = \mathrm{diag}\{\mathbb{R}_1, \ldots, \mathbb{R}_N\}$, we find that our objective function in (10) becomes

$$\frac{1}{2}\mathbf{M}^T\mathbb{W}\mathbf{M} = \mathbf{I}^T\mathbb{R}\mathbf{I} \tag{21}$$

which corresponds to the total power consumed across all dipoles, for a minimum-power solution.

For application in EMFF, there is interest in using high-temperature-superconducting (HTS) coils to enable very large currents to be used without any associated Joule heating and power loss [7], [8]. In the case of HTS coils, there is still a limit on the maximum current that can be applied to a given coil to remain in the superconducting regime, and care must be taken to avoid rapid changes in the current to mitigate the risk of quenching (rapid heating and destruction of the coils). The methods of this paper naturally address those two goals. In the scenario of interest here, in which the current flowing in a given HTS coil is being controlled in real-time, there will still be power electronics in the circuit to generate and control the current, and although the coils themselves may be cooled such that they have no electrical resistance (and thus no power loss), the power electronics for a given coil will still have an effective lumped resistance, which will result in power loss associated with current flow. In the case of HTS coils, the $\mathbb{R}$ matrix will comprise only those power-electronic resistances, without any coil resistances, but (20) is still a viable way to choose the weighting matrix.

In a distributed system in which each spacecraft carries its own power source, minimizing the total power being consumed may not be the best policy, since the failure (through depletion of power) of a single spacecraft will compromise the control of the entire system. For example, in certain scenarios a central spacecraft may be asked to generate a relatively large dipole, so that each of the surrounding spacecraft can react against it using relatively small dipoles, which will rapidly deplete the central spacecraft's energy. Our framework allows the alternate solution of weighting an individual dipole as a function of the energy currently stored in that specific spacecraft, so that a spacecraft with limited energy storage will be asked to contribute less to the combined effort.

D. Discussion

Let us now discuss a few facts that will help inform our search for an optimal solution. First, if the desired force array is $\mathbf{F}_\mathrm{d} = \mathbf{0}$, it is self-evident that the optimal solution is $\mathbf{M} = \mathbf{0}$. Second, from inspection of (8) it is easy to verify that if $\mathbf{M} \neq \mathbf{0}$ is a valid solution, then so is $-\mathbf{M}$, and both solutions will result in the same $\|\mathbf{M}\|$, so there will never be a unique global optimal solution. Consequently, it is desirable for the sake of continuity to choose whichever solution is closest to the solution from the previous time step. Third, it is easy to verify that (13) does not have a solution if $\mathbf{M} = \mathbf{0}$.

By combining the three facts above, it is clear that when transitioning from $\mathbf{F}_\mathrm{d} = \mathbf{0}$ to any other $\mathbf{F}_\mathrm{d}$, even continuously, there will not be a unique optimal solution for how to continuously transition $\mathbf{M}$ away from $\mathbf{M} = \mathbf{0}$, and the update equation (13) cannot be used in this case (at least not without modification).

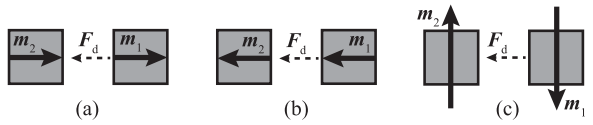

Fig. 1. Three potential dipole solutions (solid arrows) generating the same purely attractive force (dashed arrow) on dipole 1; the force on dipole 2 is equal and opposite. Solutions (a) and (b) represent optimal minimum-dipole solutions. Solution (c) and all rotations of that solution about the force vector represent suboptimal solutions that are $\sqrt{2}$ larger than optimal.

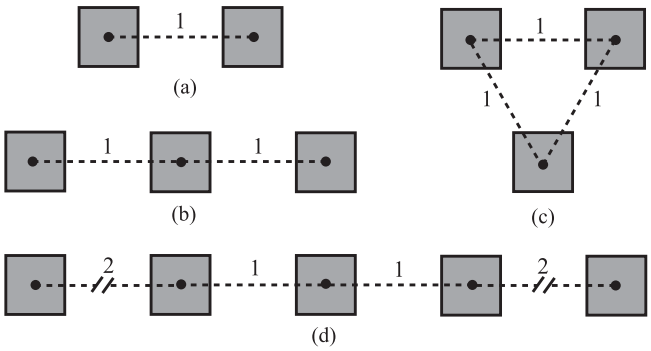

Fig. 2. EMFF scenarios considered in numerical simulations, with interdipole spacing indicated. (a) $N = 2$. (b) $N = 3$, collinear. (c) $N = 3$, equilateral triangle. (d) $N = 5$, collinear.

We must specifically address how to handle this special case. In the numerical verification in Section IV, we will simply randomly assign $\mathbf{M}[0]$ to seed our search, providing a benchmark against which future methods can be compared.

The case of $N = 2$ with $\mathbb{W} = \mathbb{I}$ is simple enough to consider a closed-form solution to our problem, and it can provide further insight into what we should expect from the general optimization. In Fig. 1, we consider the case in which the desired force is purely attractive. Fig. 1(a) and 1(b) show the two optimal solutions, each with the same $\|\mathbf{M}\|$; these solutions are intuitive, corresponding to the "north pole" of one dipole being attracted to the "south pole" of the other. Fig. 1(c) shows a suboptimal solution, with the magnitudes of the dipoles shown to scale relative to the optimal solutions; because this solution is at unstable equilibrium, being equidistant from the two optimal solutions, it could represent a solution in which our optimization routine could get stuck if sufficient steps are not taken. As we proceed forward with $N > 2$, we should be aware of these types of issues.

IV. Numerical Characterization

In this section we conduct Monte Carlo simulations to verify and characterize our method. The four cases that we consider are depicted in Fig. 2, representing the special cases of EMFF that have been explored in prior work, as described in Section I. We conduct simulations that are representative of a closed-loop regulation problem in which the set of spacecraft is trying to maintain a desired equilibrium position. Although the four equilibrium configurations lie in either a line or plane, the forces that we consider are in full 3-D.

A. Methods

We simply use $\mathbb{W} = \mathbb{I}$ so that $\mathbf{M}^T \mathbb{W} \mathbf{M} = \|\mathbf{M}\|^2$. We first generate a random desired force array $\mathbf{F}_\mathrm{d}$, where each of the elements in the arrays is chosen from a uniform distribution in the range $(-1, 1)$. This gives us a set of target forces that are nontrivial and span the space of the types of forces that might be experienced in a closed-loop regulation problem. Next, we generate a random moment array $\mathbf{M}[0]$ to seed the update equation (13), where each of the elements in the array is chosen from a uniform distribution in the range $(-10^7, 10^7)$ to counter the effect of μ_0 in (4) in order to make the update equation (13) well conditioned. This is done to mitigate the risk of converging on a local minimum that is far from a global minimum. We simply initialize the Lagrange multiplier array as $\boldsymbol{\lambda}[0] = \mathbf{0}$. We then iterate (13) until the force has converged to within 1% error of the desired force ($\|\mathbf{F} - \mathbf{F}_\mathrm{d}\|/\|\mathbf{F}_\mathrm{d}\| < 0.01$), and until the change in the dipole vector is less than 1% ($\|\Delta\mathbf{M}\|/\|\mathbf{M}\| < 0.01$). We use MATLAB's "backslash" operation to solve (13), rather than any specialized solver. We cap the number of SQP iterations allowed to 50, based on pilot testing. After convergence (or lack thereof) to a local minimum, we record the final value of $\|\mathbf{M}\|$ and the number of iterations required. Then we repeat the process with a new random $\mathbf{M}[0]$ but the same $\mathbf{F}_\mathrm{d}$, for 50 trials. We then find the minimum value of $\|\mathbf{M}\|$ from the ensemble, which is obtained by $\mathbf{M}^*$, and consider $\|\mathbf{M}^*\|$ to be the optimal value for that given $\mathbf{F}_\mathrm{d}$. We then determine the percentage of trials that converged to the optimal value by including any $\|\mathbf{M}\|$ within 1% of $\|\mathbf{M}^*\|$. We also characterize the number of iterations it took to converge to an optimal solution (minimum, mean, and maximum), in the cases that an optimal solution was found. Finally, we repeat the entire process for new randomly generated $\mathbf{F}_\mathrm{d}$, for 50 trials.

B. Results

The combined results are depicted in Fig. 3, ordered (from top to bottom) corresponding with the four cases in Fig. 2.

Considering the left column of Fig. 3, across the 50 distinct $\mathbf{F}_\mathrm{d}$ trials in each case, the mean$\pm$standard deviation in the percentage of $\mathbf{M}[0]$ that ultimately resulted in convergence to the optimal solution was as follows: $N = 2$, $46 \pm 19\%$; $N = 3$ collinear, $72 \pm 18\%$; $N = 3$ equilateral triangle, $23 \pm 12\%$; $N = 5$ collinear, $13 \pm 6\%$. We do not see a strong dependence on N, and instead the results seem to be highly configuration-dependent. We see that substantially higher percentages converge to some suboptimal solution, and upon inspection of the resulting normalized $||\mathbf{M}||$ values, we see that many of the solutions are only slightly suboptimal, falling near $||\mathbf{M}||/||\mathbf{M}^*|| = 1$ (see the right column of Fig. 3). The percentage of $\mathbf{M}[0]$ that ultimately resulted in convergence to some solution does appear to be dependent on N, with poorer convergence with increasing N.

Considering the center column of Fig. 3, of the trials that converged to the optimal value, the minimum number of iterations ever observed to converge to the optimal was quite insensitive to N: $N = 2$, 9; $N = 3$ collinear, 15; $N = 3$ equilateral triangle, 15; $N = 5$, 15. However, the median number of trials to

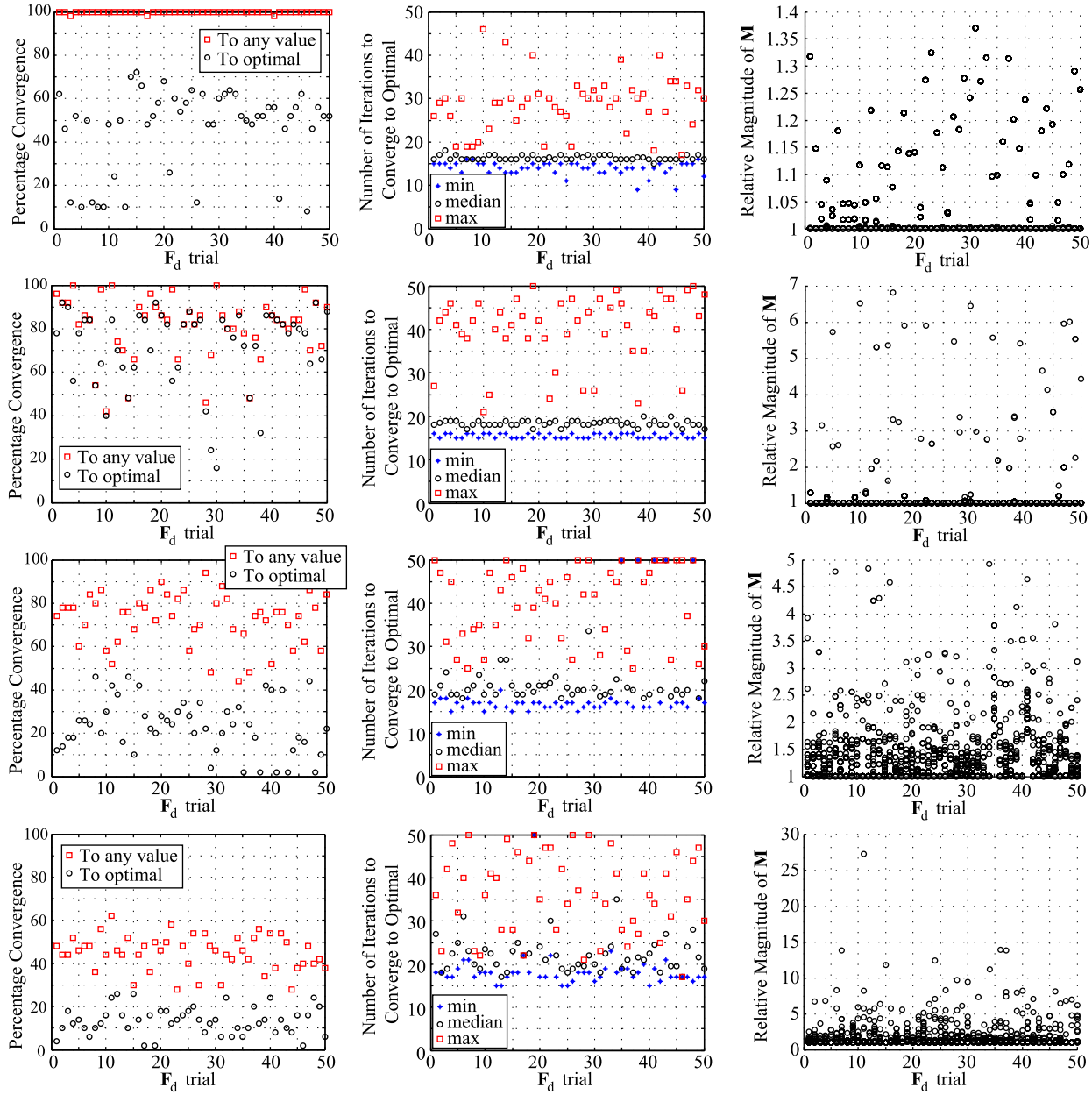

Fig. 3. Combined results of numerical simulations for the four EMFF scenarios shown in Fig. 2, which correspond to, from Top to Bottom: $N = 2$; $N = 3$, collinear; $N = 3$, equilateral triangle; $N = 5$, collinear. Left: percentage of trials that converged to any value, and percentage converged to the optimal value. Center: of the trials that converged to the optimal value (i.e., the black circles in the left column), the number of iterations required to converge. Right: magnitude of the dipole array relative to the optimal, $||\mathbf{M}||/||\mathbf{M}^*||$, for all trials that converged to any value (i.e., the red squares in the left column).

converge on the optimal is more informative and useful from an engineering perspective, since half of all future $\mathbf{M}[0]$ will converge at, or faster than, the median. We found that the median number of trials to converge on the optimal is sensitive to N. The median number of trials to converge to an optimal solution is: $N = 2$, 16; $N = 3$ collinear, 18; $N = 3$ equilateral triangle, 20; $N = 5$ collinear, 22.

C. Discussion

As discussed earlier, in cases in which we have a solution for $\mathbf{M}$ and $\boldsymbol{\lambda}$ from a prior time step, we will use those values to seed $\mathbf{M}[0]$ and $\boldsymbol{\lambda}[0]$ for the current time step. However, since we can only be assured that the prior solution corresponded to a local optimum, it would be well advised to also consider a number of random starting points, in the event that one finds a superior solution. In this way, the method can proceed with the real-time control task with a good solution (although possibly suboptimal) while the method continues to search for a better solution. The results of Fig. 3 suggest this is a viable strategy, considering a relatively high percentage of $\mathbf{M}[0]$ converge on some value, and those values are often not that suboptimal.

We have demonstrated satisfactory behavior with $N \leq 5$ dipoles in configurations relevant to EMFF, but we have not exhaustively explored other configurations, nor have we considered more dipoles. For more dipoles, or for more efficient

computation, it might be beneficial to further use mathematical structure in the optimization problem, such as the quadratic structure of the constraints and objective, to identify minimum-power solutions. In this case, one might apply global optimization methods such as convex-envelope approximations, branch and bound methods, and stochastic methods such as simulated annealing [17].

Determining the computational complexity of using SQP to solve (10) is non-trivial. Because (10) has only equality constraints with no inequality constraints, SQP is equivalent to solving a sequence of Newton-KKT systems as defined in (13). SQP is known to be quadratically convergent, provided that the starting point is sufficiently close to the optimum ([17], Ch. 18). However, the convergence rate will depend on N, and from Fig. 3 we observe that empirically the number of iterations does increase with increasing N. The computational cost to solve the $(6N-3)\times(6N-3)$ linear problem (13) at each iteration is, naively using a direct solver, $O(N^3)$, though an iterative method (e.g., conjugate gradients) with a warm start strategy will reduce this further.

It may be possible to improve our initial guess $\mathbf{M}[0]$ over choosing random numbers. For example, in the simple cases of $N=2$ depicted in Fig. 1, we can explicitly compute the optimal and suboptimal values of $\|\mathbf{M}\|$ as a function of the desired forces and the interdipole distance. It may be possible to use such a computation to seed our guess for $\mathbf{M}[0]$ in the more general case, at least in approximate magnitude, although it is currently not clear to the authors how to proceed with such a method.

V. Conclusion

We presented a method for finding a minimum-power solution for a given set of interdipole forces. We approached the optimization problem using sequential quadratic programming, which requires a Jacobain relating changes in the dipoles to changes in forces, as well as the gradient and Hessian of a Lagrangian function. We provided a compact analytic solution for all three of these quantities, which can be implemented numerically with a small set of simple functions. We conducted numerical simulations to verify the method and characterize its performance when numerical routines are randomly initialized, which can serve as a benchmark against which future improvements can be quantified.

Acknowledgment

We would like to thank D. Soloway at NASA Ames for his insight regarding electromagnetic formation flight.

References

[1] R. J. Sedwick and S. A. Schweighart, "Electromagnetic formation flight," *Adv. Astronaut. Sci.*, vol. 113, pp. 71–83, 2003.
[2] M. M. Colavita *et al.*, "Separated spacecraft interferometer concept for the new millennium program," in *Proc. SPIE.*, 1996, vol. 2807, pp. 51–58.
[3] E. M. Kong and D. W. Miller, "Optimization of separated spacecraft interferometer trajectories in the absence of a gravity-well," in *Proc. SPIE*, 1998, vol. 3350, pp. 631–643.
[4] I. I. Hussein and A. M. Bloch, "Stability and control of relative equilibria of three-spacecraft magnetically tethered systems," in *Proc. AIAA/AAS Astrodyn. Spec. Conf. Exhibit.*, 2008, pp. 1–17.
[5] H. Huang, Y. Zhu, L. Yang, and Y. Zhang, "Stability and shape analysis of relative equilibrium for three-spacecraft electromagnetic formation," *Acta Astronaut.*, vol. 94, pp. 116–131, 2014.
[6] D. W. Miller, R. J. Sedwick, E. M. C. Kong, and S. Schweighart, "Electromagnetic formation flight for sparse aperture telescopes," in *Proc. IEEE Aerosp. Conf.*, 2002, pp. 2-729–2-741.
[7] E. M. C. Kong, D. W. Kwon, S. A. Schweighart, and L. M. Elias, "Electromagnetic formation flight for multisatellite arrays," *J. Spacecraft Rockets*, vol. 41, no. 4, pp. 1–16, 2004.
[8] D. W. Kwon, "Propellantless formation flight applications using electromagnetic satellite formations," *Acta Astronaut.*, vol. 67, pp. 1189–1201, 2010.
[9] L. M. Elias, D. W. Kwon, R. J. Sedwick, and D. W. Miller, "Electromagnetic formation flight dynamics including reaction wheel gyroscopic stiffening effects," *J. Guidance, Control Dyn.*, vol. 30, no. 2, pp. 499–511, 2007.
[10] G. Zeng and M. Hu, "Finite-time control for electromagnetic satellite formations," *Acta Astronaut.*, vol. 74, pp. 120–130, 2012.
[11] W.-W. Cai, L.-P. Yang, Y.-W. Zhu, and Y.-W. Zhang, "Optimal satellite formation reconfiguration actuated by inter-satellite electromagnetic forces," *Acta Astronaut.*, vol. 89, pp. 154–165, 2013.
[12] S. Butail and M. Peck, "Non-contacting interfaces: A case study in modular spacecraft design," *Syst. Res. Forum*, vol. 2, pp. 27–34, 2007.
[13] O. Brown, P. Eremenko, and M. Bille, "Fractionated space architectures: Tracing the path to reality," in *Proc. 23rd Annu. AIAA/USU Conf. Small Satell.*, 2009, pp. 1–10.
[14] O. Brown, P. Eremenko, and P. D. Collopy, "Value-centric design methodologies for fractionated spacecraft: Progress summary from phase 1 of the DARPA System F6 program," in *Proc. AIAA SPACE Conf. Expo.*, 2009, pp. 1–14.
[15] A. J. Petruska, J. B. Brink, and J. J. Abbott, "First demonstration of a modular and reconfigurable magnetic-manipulation system," in *Proc. IEEE Int. Conf. Robot. Autom.*, 2015, pp. 149–155.
[16] S. A. Schweighart, "Electromagnetic formation flight dipole solution planning," Ph.D. dissertation, Massachusetts Inst. Technol., 2005.
[17] J. Nocedal and S. J. Wright, *Numerical Optimization*, 2nd ed. New York, NY, USA: Springer-Verlag, 2006.
[18] U. Ahsun and D. W. Miller, "Dynamics and control of electromagnetic satellite formations," in *Proc. IEEE Amer. Control Conf.*, 2006, pp. 1730–1735.
[19] Z. Xu, P. Shi, and Y. Zhao, "Optimal reconfiguration control of electromagnetic spacecraft formation using Gauss pseudospectral method," in *Proc. Int. Conf. Robot. Autom.*, 2015, pp. 862–866.
[20] A. J. Petruska, A. W. Mahoney, and J. J. Abbott, "Remote manipulation with a stationary computer-controlled magnetic dipole source," *IEEE Trans. Robot.*, vol. 30, no. 5, pp. 1222–1227, Oct. 2014.